Comparison of static and light-induced thermal hystereses of a spin-crossover solid, in a mean-field approach†

2001 J. Phys.: Condens. Matter 13 2481

(http://iopscience.iop.org/0953-8984/13/11/307)

INSTITUTE OF PHYSICS PUBLISHING JOURNAL OF PHYSICS: CONDENSED MATTER

J. Phys.: Condens. Matter **13** (2001) 2481–2495 www.iop.org/Journals/cm PII: S0953-8984(01)17852-5

Comparison of static and light-induced thermal hystereses of a spin-crossover solid, in a mean-field approach†

Cristian Enachescu[1,2], **Jorge Linarès**[1] **and François Varret**[1,3]

[1] Laboratoire de Magnétisme et d'Optique, CNRS-UMR 8634,
Université de Versailles/St Quentin en Yvelines, F78035 Versailles Cédex, France
[2] 'Alexandru Ioan Cuza' University, Faculty of Physics, Iasi, 6600, Romania

E-mail: fvarret@physique.uvsq.fr

Received 9 October 2000, in final form 19 January 2001

Abstract

We investigate the relationship between the two mean-field models which have been proposed independently for characterizing the static and the light-induced thermal hystereses of spin-transition solids, respectively involving an interaction parameter J and a relaxation self-acceleration parameter α. We unify these two models into a unique—static and dynamic—mean-field description based on Arrhenius thermal activation processes. The model is used to analyse the experimental hysteresis loops, the relaxation curves in the dark, and the light-induced instability in the spin-crossover system $[Fe_xCo_{1-x}(btr)_2(NCS)_2]H_2O$. A linear relationship between J and αT is obtained, which is in qualitative agreement with the available theories.

1. Introduction

It is already very well known that spin-transition phenomena [1–3] are related to the cooperative consequence of the thermodynamic competition between the high-spin (HS) and low-spin (LS) states of the spin-crossover molecules. The first-order entropy-driven transition is denoted here as the 'static' transition of the system. It has already been established, from the study of dilute systems [4–6], and by the analysis of earlier models [7–9], that the width of the hysteresis loop should be related to the strength of the intermolecular interactions. The precise nature of these interactions, of steric origin, remains an open question [10–12], which we do not discuss here. There is general agreement that the basic situation is a long-range interaction, which is suited to mean-field treatment. This is well explained by the elastic model introduced by Willembacher and Spiering [13]. Evidence for the presence of short-range interactions is generally scarce, but they have been detected in some cases through their static [14] or dynamic [12, 15, 16]

† This work is dedicated to the memory of our friend Olivier Kahn.
[3] Author to whom any correspondence should be addressed.

properties. A typical static model useful here, closely related to the usual solution model [9], is the Ising-like model [7, 8] with an interaction parameter denoted by J.

Cooperativity effects also influence the dynamic properties. We briefly describe a typical experiment (after [15,17,18]). At low temperature the LS state is the stable state. On irradiation causing promotion into a suitable absorption band, the molecules are switched to the metastable HS state, by the so-called LIESST effect (light-induced excited-spin-state trapping) [18–20]. Due to the onset of the HS–LS relaxation, the metastable HS state has a limited lifetime. Indeed, after photoexcitation (LIESST), the HS–LS relaxation can be measured through the high-spin-fraction curve, $n_{HS}(t)$. A sigmoidal shape of $n_{HS}(t)$ is a fingerprint of cooperativity, i.e. of the presence of interactions, and is characterized by a self-acceleration parameter α of the relaxation rate, the so-called Hauser parameter [15, 17, 21, 22]. Experiments under constant light exposure in a suitable temperature range enabled the investigation of the competition between the photoexcitation process and the relaxation of the metastable state: a thermal hysteresis under constant light irradiation was detected at low temperatures [23, 24], the so-called light-induced thermal hysteresis (LITH), and was recognized as due to self-accelerated relaxation [24, 25]. This novel aspect can be regarded as a convenient way (differential in nature) of measuring the relaxation properties.

We report here the first quantitative investigation of the relationship between the static and light-induced hystereses, i.e. between the static (J) and dynamic (α) parameters, in a mean-field approach. We first establish a single phenomenological equation which includes the static and dynamic effects. Then the experimental data for $[Fe_xCo_{1-x}(btr)_2(NCS)_2]H_2O$ [5, 6, 24, 26, 27] are analysed and discussed.

2. Mean-field models

2.1. The static Ising-like model (after [28])

The simple Ising Hamiltonian is

$$H = \sum_i \frac{\Delta_0}{2}\sigma_i - J\sum_{\langle i,j\rangle}\sigma_i\sigma_j \tag{1}$$

where Δ_0 is the electronic gap between LS and HS states; σ_i and σ_j are fictitious spin operators with eigenvalues ± 1, respectively associated with the HS, LS spin states, with degeneracies g_{HS}, g_{LS}; J is the interaction parameter (identical first neighbours). In the uniform mean-field approach the one-site Hamiltonian is

$$H_i = \frac{\Delta_0}{2}\sigma_i - J\sigma_i\langle\sigma\rangle \tag{2}$$

with J now including the number of neighbours. The energy values are

$$E_{HS} = \frac{\Delta_0}{2} - J\langle\sigma\rangle \tag{3}$$

$$E_{LS} = -\frac{\Delta_0}{2} + J\langle\sigma\rangle. \tag{4}$$

Thus, the mean-field view of the Ising system is that of independent two-level systems with an energy gap depending on the order parameter $\langle\sigma\rangle$, as follows:

$$\Delta = E_{HS} - E_{LS} = \Delta_0 - 2J\langle\sigma\rangle. \tag{5}$$

- In the spin-transition community, the commonly used order parameter is the high-spin fraction n_{HS}, the relative number of molecules in the HS state, such that

$$n_{HS} = \frac{1+\langle\sigma\rangle}{2} \tag{6}$$

and, consequently,

$$\Delta(n_{HS}) = \Delta_0 - 4Jn_{HS} + 2J = \Delta(0) - 4Jn_{HS}. \tag{7}$$

$\Delta_0 = \Delta(n_{HS} = 1/2)$ is the single-molecule contribution to the enthalpy change upon spin conversion; $\Delta_0 = \Delta H/N_0$ with ΔH the enthalpy change upon spin transition of one mole, and N_0 Avogadro's number. The mean-field treatment of the Ising-like model is equivalent to the (generally used) usual solution thermodynamical model [9], with the additional relationships $\Delta S = k_B \ln g_{HS}/g_{LS}$, $\Gamma = 2J$ [29].

In terms of the molecular configurational diagram, figure 1, the cooperative effect can be introduced, in a first approach suggested by equation (7), as a change in the energy difference between the wells associated with the two spin states, i.e. as a vertical shift of the energy wells: with positive J, on increasing (decreasing) the population of the HS state, the HS well is stabilized (destabilized). The same holds for the LS well. This is a way to illustrate how cooperativity ($J > 0$) induces a *static stabilization of the populated state*, which enhances the effect of the spontaneous thermal population of the isolated molecule, and finally may transform a continuous thermal population effect into a first-order transition.

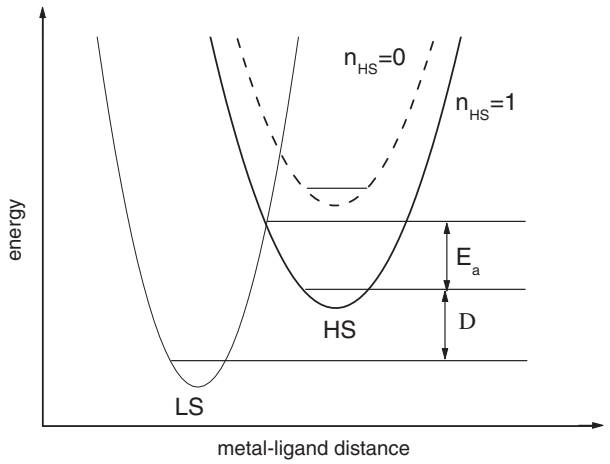

Figure 1. The configuration diagram of a spin-crossover molecule, i.e. the adiabatic energies of the lowest vibronic state, in each spin state, as a function of the metal–ligand distance (after [2]). The static and dynamic effects of cooperativity are illustrated: on populating the HS state, its relative energy decreases and its energy barrier is increased.

In this Ising-like model, the two states have different degeneracies, because of the different spin multiplicities and of the different vibrational properties associated with the two spin states [28,30]. Indeed, the entropy change upon conversion ΔS is often quite large and contains prominent vibrational contributions [31, 32]. Accordingly, a large value has to be attributed to the 'effective' degeneracy ratio, $g = g_{HS}/g_{LS} = \exp(\Delta S/R)$, which can be expressed approximatively as the product of the electronic ratio and of the densities of the low-energy vibrational states [30]. Because of the vibrational contribution, the effective degeneracy ratio is highly system dependent and, in the present case, concentration dependent. A slight thermal dependence of the effective degeneracy ratio has been detected [33], and it may be sizable when $\Delta \sim 0$; then the conversion curve is mainly governed by the vibrational properties [30,34]. For simplicity, the present model includes temperature-independent ΔS, ΔH, obviously related to the equilibrium temperature through $\Delta H = T_{equil}\,\Delta S$.

The canonical analysis yields the following self-consistent equation:

$$\langle\sigma\rangle = \frac{g_{HS}\,\mathrm{e}^{-E_{HS}/(k_BT)} - g_{LS}\,\mathrm{e}^{-E_{LS}/(k_BT)}}{g_{HS}\,\mathrm{e}^{-E_{HS}/(k_BT)} + g_{LS}\,\mathrm{e}^{-E_{LS}/(k_BT)}}. \tag{8}$$

The self-consistent equation (8) is expressed also in terms of the HS fraction, as usual:

$$n_{HS} = \frac{g}{g + \mathrm{e}^{\Delta(n_{HS})/(k_BT)}} \tag{9}$$

or, equivalently,

$$\frac{n_{HS}}{n_{LS}} = g\mathrm{e}^{-\Delta(n_{HS})/(k_BT)}. \tag{10}$$

The equilibrium temperature (such that $n_{HS} = n_{LS} = 1/2$) is deduced, irrespective of the interaction parameter, as

$$T_{equil} = \frac{\Delta}{k_B \ln g}. \tag{11}$$

It is worth noting that the Ising-like model is formally equivalent to a 'true' Ising model (no degeneracies) under a temperature-dependent field [35] which accounts for the effect of the degeneracies. Equation (10) is rewritten as

$$\frac{n_{HS}}{n_{LS}} = \mathrm{e}^{-\Delta_{eff}(n_{HS})/(k_BT)}$$

with the temperature-dependent effective field

$$\Delta_{eff}(n_{HS}, T) = \Delta(0) - 4Jn_{HS} - k_BT \ln g. \tag{12}$$

So, the temperature acts as a field, which goes to zero at T_{equil}, thus giving rise to the first-order transition, at $T = T_{equil}$, provided that the pure Ising system is ordered [35–37], i.e. for $J > k_BT_{equil}$, in the mean-field approach.

2.2. Cooperative relaxation

The HS $\rightarrow$ LS relaxation was first investigated by Hauser with the Mainz group [15, 18, 22]. The following discussion, therefore, is based on their analysis of the properties of the energy barrier of the high-spin state: since the energy gap $\Delta = E(\mathrm{HS}) - E(\mathrm{LS})$ is a decreasing function of n_{HS} (see the previous section, figure 1), the height of the energy barrier is expected to be an increasing function of n_{HS}; this leads to a self-accelerated relaxation for the spontaneous decrease of n_{HS}: at the beginning of the relaxation process ($n_{HS} \simeq 1$, small gap Δ, large energy barrier), the relaxation is slow; then it becomes faster and faster (decreasing n_{HS}, increasing gap, lowering energy barrier). This cooperative dynamic effect is easily generalized: the increased (decreased) population of a given state induces an increase (decrease) of its lifetime; in other words it increases (decreases) the 'dynamic stability' of the state. Thus the static and dynamic effects of cooperativity are similar in nature: increasing the population of a given state increases both its static and 'dynamic' stability. The effect applies also in the (high-temperature) thermal activation regime and in the (low-temperature) tunnelling regime.

A useful expression for the relaxation rate k_{HL} was given by Hauser [18, 22], both on experimental and theoretical bases. They considered a linear dependence of the barrier energy versus n_{HS}. In the thermal activation regime, the relaxation rate is expressed as

$$k_{HL}(n_{HS}, T) = k_\infty \exp\left(-\frac{E_a(n_{HS})}{k_BT}\right) \tag{13}$$

with

$$E_a(n_{HS}) = E_a(0) + an_{HS} \tag{14}$$

where E_a is the activation energy, a is a term of cooperative origin, k_∞ is the high-temperature rate (associated with some vibrational frequencies), and k_B is the Boltzmann constant. Equation (13) is rewritten as

$$k_{HL}(n_{HS}, T) = k_\infty \exp\left(-\frac{E_a(0) + an_{HS}}{k_B T}\right) = k_\infty \exp\left(-\frac{E_a(0)}{k_B T}\right) \exp(-\alpha(T) n_{HS}) \tag{15}$$

where $\alpha(T)$ is the self-acceleration factor. In the uniform-dilution mean-field approach, the cooperative coefficient a can be assumed to be proportional to Jx, with J the interaction constant in the pure system and x the dilution factor of the spin-crossover atoms. The following relation is derived [15, 25]:

$$\alpha(x, T) = A\frac{x}{T} \tag{16}$$

in agreement with the previous relation $\alpha T = \Gamma\ (=2Jx)$ [17] derived from the elastic model of Willembacher and Spiering [13] and also obtained in a recent dynamical Ising model study [37]. It is worth noting that the proportionality between α and the cooperativity parameter (Γ or J) has been controlled experimentally for several systems [24, 38]. Such a proportionality seems to hold, irrespectively of the actual relaxation regime, i.e. tunnelling, thermally assisted tunnelling, or 'classical' thermal activation [42].

2.3. The dynamical macroscopic model

We now consider both the HS $\rightarrow$ LS and LS $\rightarrow$ HS processes, in order to obtain a dynamical equation valid up to the transition temperature. The relaxation rates k_{HL}, k_{LH}, i.e. the transition rates for a molecule for switching spontaneously from HS to LS and from LS to HS respectively, obey the detailed-balance equation:

$$k_{HL}(n_{HS}, T) n_{HS}^{equil}(T) = k_{LH}(n_{HS}, T) n_{LS}^{equil}(T). \tag{17}$$

The detailed-balance equation enables us to derive k_{LH} from k_{HL}, once the static properties are known. This is easily done using equation (10), as follows:

$$\frac{k_{LH}}{k_{HL}} = \left(\frac{n_{HS}}{n_{LS}}\right)_{equil} = g \exp\left(-\frac{\Delta(n_{HS})}{k_B T}\right). \tag{18}$$

The dynamic properties of a system, in the general case, are governed by the master equation (ME), i.e. the evolution equation. It is written in the macroscopic form given in [24, 25], including a constant-photoexcitation term, completed here for the spontaneous LS $\rightarrow$ HS relaxation:

$$\frac{\mathrm{d}n_{HS}}{\mathrm{d}t} = I_0\sigma(1 - n_{HS}) - k_{HL} n_{HS} + k_{LH}(1 - n_{HS}) \tag{19}$$

where $I_0\sigma$ is the transition rate for a molecule being switched by the light from the LS to the HS state, I_0 is the intensity of the radiation, and σ is a proportionality coefficient which depends on the cross section and on the number of absorbing atoms.

Inserting the expressions for k_{HL} and k_{LH}, the ME (equation (19)) becomes, in the framework of the thermal activation regime,

$$\begin{aligned}\frac{\mathrm{d}n_{HS}}{\mathrm{d}t} = {} & I_0\sigma(1 - n_{HS}) - k_\infty n_{HS} \exp\left(-\alpha n_{HS} - \frac{E_a(0)}{k_B T}\right) \\ & + k_\infty g(1 - n_{HS}) \exp\left(-\alpha n_{HS} - \frac{E_a(0)}{k_B T}\right) \exp\left(-\frac{\Delta(n_{HS})}{k_B T}\right).\end{aligned} \tag{20}$$

For convenience we shall mostly refer to the activation energy in the equilibrium situation, $E_a(n_{HS} = 1/2) = E_a(0) + \alpha k_B T/2$, which is that of non-interacting molecules, i.e. the energy

barrier associated with the energy gap Δ_0. The straightforward transformation of the above equation (20) is not reported here. It must be noted that α is proportional to the inverse temperature and $\Delta(n_{HS})$ contains the static cooperativity parameter J. The state equation for the steady states (i.e. photostationary states under constant experimental conditions) is straightforwardly derived by setting $\mathrm{d}n_{HS}/\mathrm{d}t = 0$. This can be resolved analytically via the explicit expression of T.

Under a constant photoexcitation, it is obvious that the low-temperature steady state is a high-spin one (slow HS $\rightarrow$ LS relaxation); on increasing the temperature, since the relaxation becomes faster, the photostationary state exhibits a spin equilibrium, with a HS fraction which is a decreasing function of temperature. A light-induced equilibrium temperature ($n_{HS} = 1/2$) follows, and the crucial point is the stability of the corresponding steady state. Due to the presence of non-linear terms in the master equation, the equilibrium steady state may become unstable, hence leading to there being hysteresis loops—the so-called LITH and LIOH loops, standing for thermal and optical hystereses, after [23–25].

At low temperature, neglecting k_{LH} in comparison to k_{HL}, the steady states, derived from equation (20), are expressed as follows:

$$\left(\frac{n_{HS}}{n_{LS}}\right)_{steady\,state} = \frac{I_0\sigma}{k_\infty}\exp\left(\frac{E_a(n_{HS})}{k_BT}\right). \tag{21}$$

Here again, the role of temperature can be likened to that of a field. A temperature-dependent effective field is derived from the transformation of equation (21):

$$\left(\frac{n_{HS}}{n_{LS}}\right)_{steady\,state} = \exp\left(-\frac{\Delta^*_{eff}(n_{HS})}{k_BT}\right).$$

The light-induced temperature-dependent field is expressed as

$$\Delta^*_{eff}(n_{HS}, I_0, T) = k_BT\ln\frac{k_\infty}{I_0\sigma} - E_a(n_{HS}). \tag{22}$$

Since $k_\infty \ggg I_0\sigma$ (at high temperatures, relaxation overcomes photoexcitation), Δ^*_{eff} is an increasing function of temperature, which passes through zero at T^*_{equil}. The light-induced equilibrium temperature is expressed as

$$T^*_{equil} = \frac{E_a(n_{HS} = \frac{1}{2})}{k_B\ln(k_\infty/[I_0\sigma])}. \tag{23}$$

In the general case, numerical solution of the steady-state and master equations is needed, except for the static transition, which can be treated using the explicit expression for $T(n_{HS})$.

We have also considered the effect of light on the static transition. For this, k_{LH} is no longer neglected in comparison to k_{HL} in the master equation (20) and the following equation for the steady states is obtained:

$$\frac{I_0\sigma}{k_\infty} = \exp\left(-\frac{E_a(1/2)}{k_BT}\right) - g\exp\left(-\frac{E_a(1/2)+\Delta_0}{k_BT}\right). \tag{24}$$

Equation (24), above, has up to two solutions: the low-temperature one is the light-induced equilibrium temperature already expressed—approximatively—by equation (23). The high-temperature solution can be estimated by calculating the derivative of I_0 with respect to T. The light-induced shift of the static transition is—again approximatively—expressed as

$$\Delta T_{equil} = -\frac{k_BT^2_{equil}}{\Delta_0}\frac{I_0\sigma}{k_\infty}\exp\left(\frac{E_a(1/2)}{k_BT}\right). \tag{25}$$

The above expression is valid to first order in $I_0\sigma/k_\infty$. On increasing the intensity factor, the two solutions of (24) move towards each other, and a collapse of the solutions can be expected. Large intensity values prevent the system from reaching the low-spin state, at any temperature.

2.4. Experimental data and simulation

The spin-crossover solids $[Fe_xCo_{1-x}(btr)_2(NCS)_2]H_2O$, denoted as [Fe($x$)], present a thermal hysteresis for $x > 0.4$. In [5, 6, 26, 27], the temperature–composition phase diagram has been established, and showed linear dependences of T_{equil}, $T_{c\downarrow}$, $T_{c\uparrow}$ versus x, where these temperatures respectively are the equilibrium temperature and the static transition temperatures in the heating and cooling modes. Useful data are collected in table 1.

Table 1. The thermodynamic data after [5, 6], revisited by [26, 27], and the derived parameters for the system $[Fe_xCo_{1-x}(btr)_2(NCS)_2]H_2O$.

x	ΔH (J mol^{-1})	ΔS (J mol^{-1} K^{-1})	T_{equil} (K)	$T_{c\downarrow}$ (K)	$T_{c\uparrow}$ (K)	g	Δ_0 (K)
0.3	4978	50.1	99.34	—	—	416	598
0.5	6430	58.8	—	106.5	111.5	1187	773
0.85	8971	70.7	—	116.6	134.6	4985	1080

The compositions selected here belong to the composition range for which both the LIESST and LITH effects could be obtained. Below $x = 0.3$, cooperativity is so weak that no hysteresis is observed—neither spontaneous, nor photoinduced. Above $x = 0.85$, e.g. for $x = 1$, the LITH loop is expected to be extremely wide, with a low-temperature branch leading to extremely slow kinetics, out of reach with the available liquid-helium device (SQUID + optical access). In addition, previous experiments showed that the LIESST effect was hardly obtained with $x = 1$, presumably because the stronger cooperativity results in a large intensity threshold effect, as described in [24].

The thermodynamic data of table 1 enable us to determine the degeneracy ratio $g = \exp(\Delta S/R)$ and the energy gap $\Delta_0 = T_{equil}\,\Delta S/N_A$ (with N_A the Avogadro number) for all three compositions.

The static data are taken from [5,6,26,27], obtained from the magnetization measurements in a SQUID magnetometer, and Mössbauer spectroscopy. We determined, numerically, the J-values associated with the width of the static hysteresis loops, using the present mean-field model. For the most dilute compound ($x = 0.3$), which does not show a static hysteresis, the smooth shape of the conversion curve $n_{HS}(T)$ was analysed instead. The so-determined J-values are collected in table 2.

Table 2. Cooperativity parameters J and αT (both in temperature units), derived parameter, and thermodynamic parameter values deduced from the relaxation and light-induced data.

x	J (K)	J/x (K)	αT (K)	$\alpha T/J$	$E_a(1/2)$ (K)	$k_{\rm inf}$ (s^{-1})	αT_{LITH} (K)	$I_0\sigma$ (s^{-1})	$\alpha T_{LITH}/J$
0.3	53	180	86	1.6	490	10	160	0.0018	3.0
0.5	136	272	262	2.0	579	90	350	0.0024	2.6
0.85	208	244	412	2.0	660	3850	507	0.0021	2.4

2.5. Experimental relaxation data

Relaxation curves have been obtained after LIESST using a 550 nm wavelength, with typical intensity 30 mW cm^{-2}. The data for $x = 0.50$, 0.85 were taken from [26], and are completed by new data for $x = 0.30$, obtained using the same SQUID magnetometer equipped with an optical fibre. The experimental data, with the curves calculated in the present analysis, are reported in figure 2.

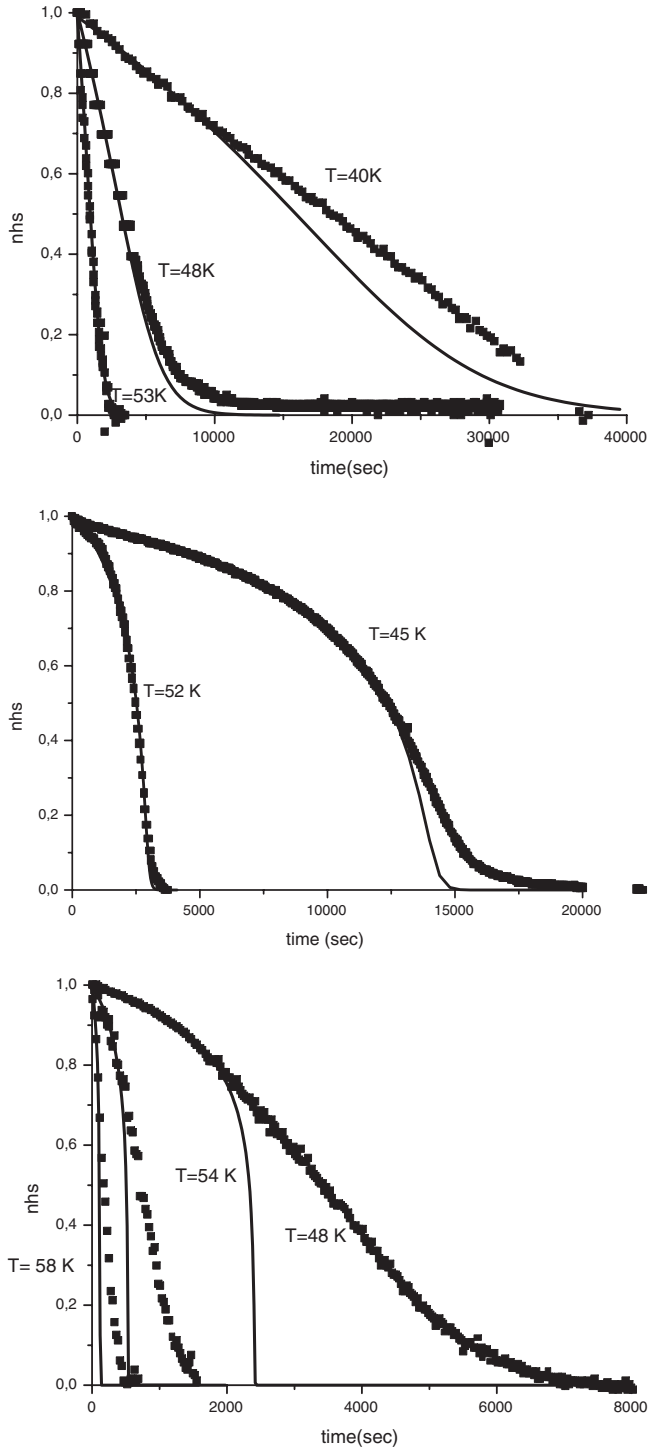

Figure 2. Experimental relaxation curves after photoexcitation (squares), and (best-fit) curves computed in the present approach. Notice the so-called 'tail effect', i.e. the departure from the model, for long times, varying according to the strength of the cooperativity and the temperature.

Some fitted curves have been previously presented in [24] which illustrated the 'tail effect'—i.e. the extra slowing down of relaxation at long times and in concentrated systems. The tail effect was first described and analysed by Hauser and the Mainz group as due to the progressive onset of short-range correlations [10, 39]. These correlations introduce additional energy barriers for the relaxation process [40]. An alternative mechanism possibly responsible for the onset of the tail is a spreading of the barrier energies [38, 41, 42]. This is not likely here, due to the obvious correlation between the amplitude of the tail and the composition parameter x.

Due to the presence of the tail effect, which is quite large in some cases, we have carried out a very careful and stepwise analysis of the data, as follows:

(i) We have transformed the $n_{HS}(t)$ data into $k_{HL}(n_{HS})$, for each composition and at each temperature, according to the basic relationship $k_{HL} = -\mathrm{d}(\ln n_{HS}(t))/\mathrm{d}t$; the numerical derivation was followed by a (slight) smoothing process; typical $k_{HL}(n_{HS})$ data are reported in figure 3.

(ii) According to equation (15), in the mean-field approach, a linear plot of $\ln k_{HL}(n_{HS})$ versus n_{HS} is expected, expressed as

$$\ln k_{HL}(n_{HS}) = \ln k_{HL}(0) - \alpha n_{HS}. \tag{26}$$

Actually, all data display a rather complex variation, with the expected decreasing linear plot within a limited range of n_{HS}-values only. The head of the relaxation curves may exhibit a short transient regime, in the shape of a stretched exponential, associated with a distribution of relaxation times which we explained as the effect of cooperative relaxation on a slightly inhomogeneous initial state (for instance due to bulk absorption of light in the sample [43]). This can be shown as an extra increase in the right-hand part of the curves in figure 3. On the other hand, the tail effect obviously results in an extra lowering of the data at long times, i.e. on the left-hand side of the curves in figure 3. The combination of these effects gave the experimental curves a typical wavy shape, and understanding this enabled us to select the useful (linear) part of the data. Obviously, the selected range of n_{HS}-values was rather small for the more cooperative sample ($x = 0.85$) and at the lower temperatures, but it was however sufficient for performing a linear regression. Thus, for each sample, at each temperature, $\alpha(T)$ and $k_{HL}(0, T)$ could be determined.

(iii) Remarkably, the values obtained for $\alpha(T)$ follow with an excellent accuracy the expected dependence $\alpha(T)T = \text{constant}$, so we have merely reported in table 2 the average values of this product, for each sample. On the other hand, the relaxation rates are consistent with the relation $k_{HL}(0, T) = k_\infty \mathrm{e}^{-E_a(0)/(k_B T)}$ expected in the thermal activation regime. We show in figure 4 the Arrhenius plots, i.e. the plots of $\ln k_{HL}(0, T) = \ln k_\infty - E_a/k_B T$ versus $1/T$, the linear regressions of which allow the determination of the spin-flip frequency k_∞ and of the barrier energy $E_a(0)$ for each sample. The barrier energy is better reported at equilibrium, since $E_a(1/2)$ characterizes the intrinsic properties of the (isolated) spin-crossover units. These data are collected in table 2.

A brief inspection of table 2 immediately makes us aware that the k_∞-values are unrealistically low, in comparison to the expected orders of magnitude, 10^{10} to 10^{12} s^{-1}. This discrepancy is attributed to the relaxation regime, which is closer to the tunnelling mechanism than to the thermal activation mechanism in the experimental temperature range [42]. Therefore, the measured activation energies are obviously underestimated, and should not be discussed further; they can only be considered as 'apparent' activation energies, for the phenomenological description of the thermal dependence of the relaxation rates. The situation for the α-values is totally different. Indeed, theoretical α-values given by the multi-phononic adiabatic approach of Hauser *et al* [42] seem to follow closely the thermal activation

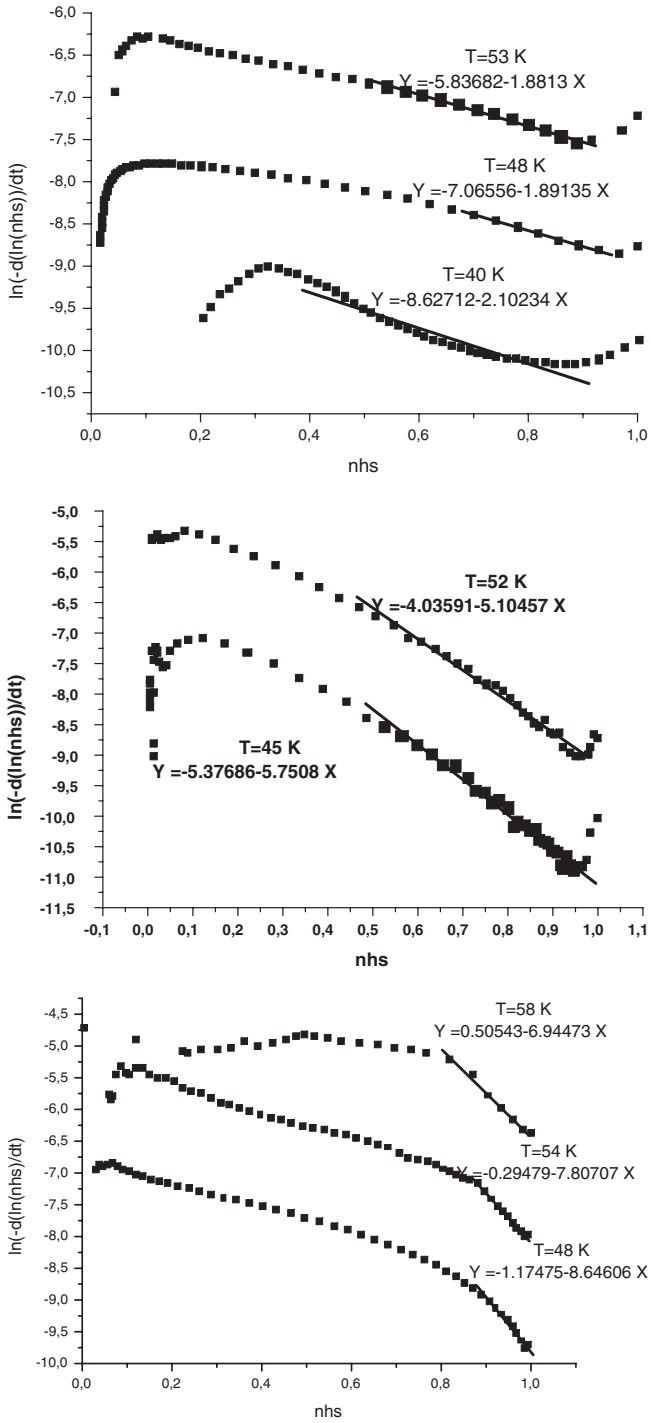

Figure 3. Typical plots for the analysis of the relaxation curves: n_{HS}-dependences of the relaxation rates $k_{HL} = -\mathrm{d}\ln(n_{HS})/\mathrm{d}t$. The linear regressions were performed over selected ranges of n_{HS}-values, as shown by the straight lines. The self-acceleration parameters $\alpha(T)$ are given by the slopes of the straight lines.

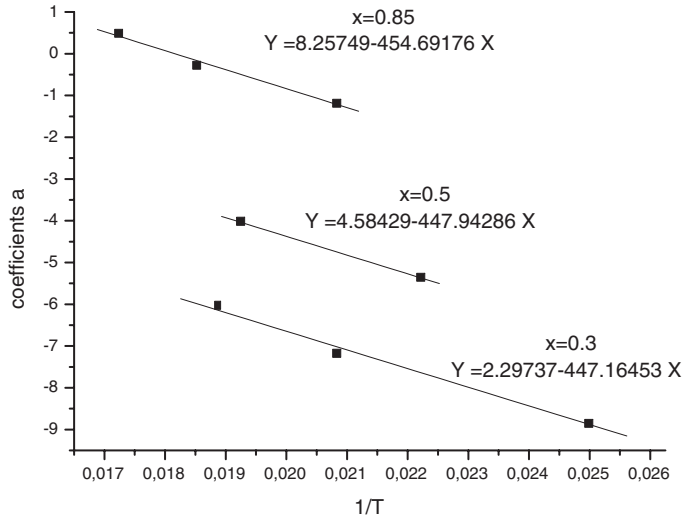

Figure 4. Arrhenius plots, for all samples, of $\ln(k_{HL}(n_{HS} = 0)) = \ln(k_{\inf}) - E(0)/T$.

model down to lower temperatures, before they undergo a rapid crossover to the temperature-independent tunnelling regime. Consequently, the experimental α-values can be discussed here as significant physical data, associated with the thermal activation regime.

2.6. Experimental LITH loops

We show in figure 5 the experimental data on the high-spin fraction under constant excitation, taken from [24]. The experimental kinetics is rather slow (the typical total time for achieving the loop was between 12 and 24 hours), and the data can be considered as being close to the quasi-static state (steady state) [41, 43]. As we suggested in previous works, we have selected the optical data (reflected intensity/incident intensity ratio), which are less affected by the effect of bulk absorption of light than are the magnetic data.

However, the optical curves still depart substantially from the expected shapes: the edges are not sharp, presumably because the bulk absorption and kinetic effects are not totally negligible. The kinetic effects are due to the limited experimental time. Bulk absorption occurs in the rather thin layer which contributes to the reflected intensity. Both a non-null kinetics ($\mathrm{d}T/\mathrm{d}t$) and a non-uniform intensity [44], due to bulk absorption as well as the bleaching effects, should be systematically considered for an accurate reproduction of the experimental loop.

It is also worth noting that optical measurements induce photoexcitation of the sample, which may be sizable at low temperature, when the relaxation is not fast enough to depopulate the metastable state. Therefore optical measurements could not be used for recording the (spontaneous) relaxation of the metastable state, which had to be followed, in the dark, by magnetic measurements.

We have reported in figure 5 the computed solutions of the steady-state equation. We used the dynamic parameter values extracted from the relaxation curves, i.e. those reported in table 2. The only parameter needed, in principle, for matching the experimental LITH loops, was the intensity parameter $I_0\sigma$, which is difficult to accurately control at the experimental level. We also found it necessary to substantially increase the values of the cooperativity parameter αT,

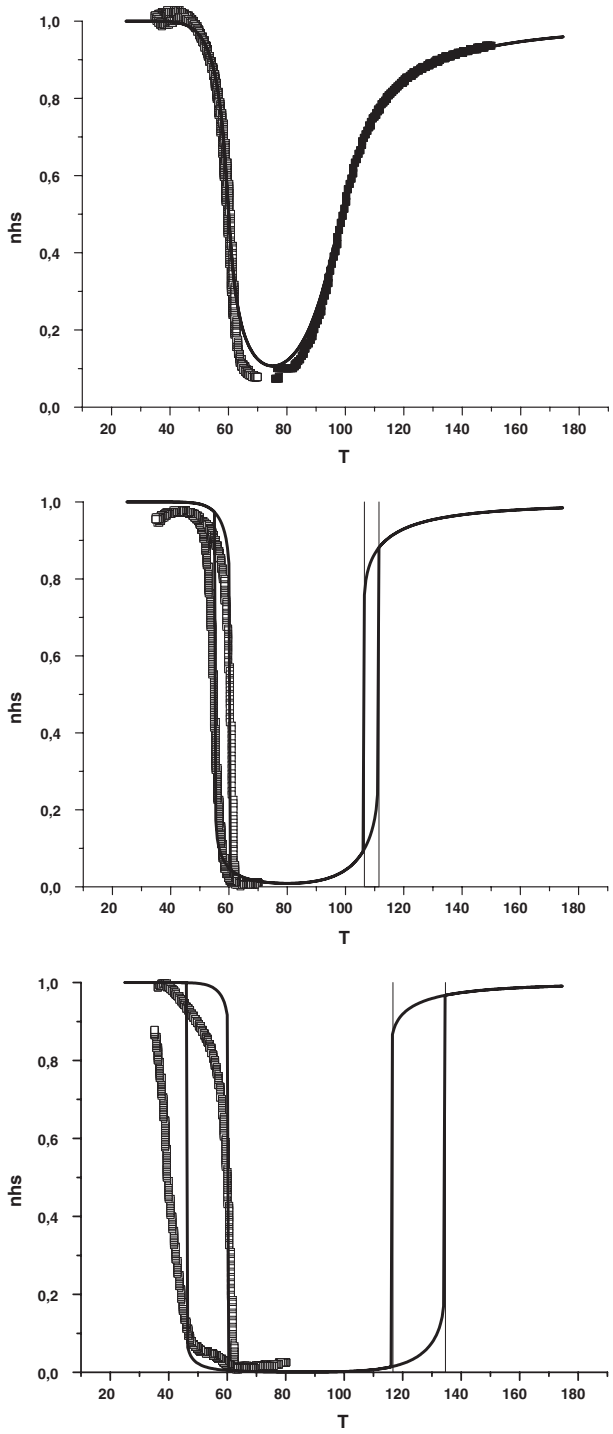

Figure 5. Conversion curves, $n_{HS}(T)$, for a slow temperature sweep under constant irradiation: experiments (squares, taken from [24]) and computed steady-state curves, using parameter values listed in table 2. The high- and low-temperature loops are respectively the spontaneous and the LITH loops.

with respect to the relaxation data. We have chosen to obtain an exact matching in the bottom part of the LITH loop (smaller n_{HS}-values), because it corresponds to the fastest relaxation rate and a higher intensity, so as to minimize both of the experimental effects reported above. Indeed, this part of the loop is clearly that of greatest slope, in better agreement with the expected vertical edges of the theoretical LITH loop.

We have also estimated the effect of light on the static equilibrium temperature. Using equation (25), and reasonable data ($k_\infty = 10^{11}$ s^{-1}, $E_a(1/2) = 1000$ K, $\Delta = 800$ K), we obtained $\Delta T_{equil} = -10^{-9}$ K. Obviously, the photoexcitation effect is negligible at the temperature of the static hysteresis loop, in agreement with a previous observation [43] that the optical measurements as well as the magnetic measurements are suited to monitoring the static spin transition. In other words, the high-temperature relaxation widely overcomes the photoexcitation, with the available light intensity.

3. Discussion and conclusions

The fitted data relating to the static and light-induced thermal hysteresis loops are collected in table 2. For an easier comparison of the cooperative effect parameters, we have calculated the values of J/x and $\alpha T/J$, which are expected to be constant within the framework of the available mean-field models quoted here.

It is worth noting that the static parameter J is not obtained as exactly proportional to the iron composition parameter x, as it would be in the uniform-dilution mean-field approach. This was already remarked in [27] and led to the introduction of second-neighbour interactions.

It is also remarkable that the mean-field model reproduces rather well the shape of the LITH curves, while it fails to reproduce the tail of the relaxation curves. This could be due to the effect of light, which excites at random the spin-crossover molecules, and therefore hinders the building up of the correlations [16]. However, the agreement between the cooperativity parameters αT, derived from the sigmoidal part of the relaxation curves and from the LITH loops, is not perfect, and thus suggests that the effect of short-range interactions is sizable, even before the development of the tail.

The main point to be discussed here is the proportionality between the two parameters J and αT, which seems to be qualitatively obeyed, within the framework of the approximations involved in the phenomenological approaches that we used. Of course, this is the first system investigated so far from this viewpoint, and the drawbacks of the models are obvious. Therefore it would be unrealistic to attempt to derive a general conclusion in accurate quantitative terms. However, tentatively, the range of values for the ratio $\alpha T/J \simeq 2.0$ (relaxation)–2.5 (LITH) compares well to the available theoretical prediction $\alpha T = 2J$ [17, 37] (irrespective of the ligand-field strength and of the degeneracy ratio).

The present analysis is obviously limited by the shortcomings of the mean-field approach. The sizable discrepancy between the relaxation and light-induced data is probably due to the effect of short-range interactions, which may affect the sigmoidal part of the relaxation curve in addition to the development of the tail of the curves. A model combining the first-neighbour correlations [40,45] and the multiphononic approach to the relaxation [22,42,46,47] remains to be constructed. The open question of the range of interactions in the spin-crossover solids (see [48, 49] for a discussion) should be answered thanks to the combined analysis of relaxation curves (including the tail) and light-induced effects. It should also be mentioned that some recent experiments, with very large light intensities, have evidenced a collective photoexcitation, according to the so-called 'domino effect' [50], which also depends on the role of the short-range interactions.

An interesting perspective is that of the possible collapse between the two hysteresis loops, at large photoexcitation rates. Experimental effort should be devoted to this fascinating situation, which requires either a higher intensity (experimentally difficult), or the use of more efficient metal-to-ligand charge-transfer bands [51]. Also, a lower spin-transition temperature would help in reaching the collapse situation.

Acknowledgments

We are grateful to Dr K Boukheddaden and to B Hoo for fruitful discussions and for communicating their theoretical results prior to publication, and to Professor Andreas Hauser for helpful discussion. The work was supported by the European Community: TMR contract ('TOSS' ERB-FMRX-CT98-0199) and the Socrates programme (Cristian Enachescu was on a Socrates grant).

References

[1] Gütlich P 1981 *Struct. Bonding* **44** 83
[2] König E 1991 *Struct. Bonding* **76** 51
[3] Kahn O 1993 *Molecular Magnetism* (New York: VCH)
[4] Spiering H, Meissner E, Köppen H, Müller E W and Gütlich P 1982 *Chem. Phys.* **68** 65
[5] Martin J P 1993 *PhD Thesis* Université Paris-Sud
[6] Martin J P, Zarembowitch J, Bousseksou A, Dworkin A, Haasnoot J P and Varret F 1994 *Inorg. Chem.* **18** 2617
[7] Wajnsflasz J and Pick R 1971 *J. Phyique Coll.* **32** C1 91
[8] Bousseksou A, Nasser J, Linarès J, Boukheddaden K and Varret F 1993 *Mol. Cryst. Liq. Cryst.* **234** 269
[9] Slichter C P and Drickamer H G 1972 *J. Chem. Phys.* **56** 2142
[10] Romstedt H, Spiering H and Gütlich P 1998 *J. Phys. Chem. Solids* **59** 1353
[11] Bolvin H and Kahn O 1993 *Mol. Cryst. Liq. Cryst.* **234** 257
[12] Spiering H 1999 *Coord. Chem. Rev.* **190–192** 629
[13] Willembacher N and Spiering H 1988 *J. Phys. C: Solid State Phys.* **21** 1423
[14] Real J A, Bolvin H, Bousseksou A, Dworkin A, Kahn O, Varret F and Zarembowitch J 1992 *J. Am. Chem. Soc.* **114** 4650
[15] Hauser A, Gütlich P and Spiering H 1986 *Inorg. Chem.* **25** 4345
[16] Hauser A 1997 *J. Phys. Chem. Solids* **59** 265
[17] Adler P, Hauser A, Vef A, Spiering H and Gütlich P 1989 *Hyperfine Interact.* **47** 343
[18] Hauser A 1991 *J. Chem. Phys.* **94** 2741
[19] Decurtins S, Gütlich P, Köhler C P, Spiering H and Hauser A 1984 *Chem. Phys. Lett.* **1** 139
[20] Gütlich P, Hauser A and Spiering H 1994 *Angew. Chem. Int. Edn Engl.* **33** 2024
[21] Hauser A, Vef A and Adler P 1991 *J. Chem. Phys.* **95** 8710
[22] Hauser A 1992 *Chem. Phys. Lett.* **192** 65
[23] Létard J F, Guionneau P, Rabardel L, Howard J A K, Goeta A E, Chasseau D and Kahn O 1998 *Inorg. Chem.* **37** 4432
[24] Desaix A, Roubeau O, Jeftic J, Haasnoot J G, Boukheddaden K, Codjovi E, Linarès J, Nogués M and Varret F 1998 *Eur. Phys. J.* B **6** 183
[25] Varret F, Boukheddaden K, Jeftic J and Roubeau O 1999 *Proc. ICMM '98 (Seignosse, France); Mol. Cryst. Liq. Cryst.* **335** 561
[26] Constant-Machado H 1997 *PhD Thesis* Université Paris-6
[27] Constant-Machado H, Linarès J, Varret F, Haasnoot J, Martin J P, Zarembowitch J, Dworkin A and Bousseksou A 1996 *J. Physique* I **6** 1203
[28] Bousseksou A, Varret F and Nasser J 1993 *J. Physique* **3** 1463
[29] Zimmermann R and König E 1977 *J. Phys. Chem. Solids* **38** 779
[30] Bousseksou A, Constant-Machado H and Varret F 1995 *J. Physique* I **5** 747
[31] Sorai M and Seki S 1974 *J. Phys. Chem. Solids* **35** 5550
[32] Bousseksou A, McGarvey J, Varret F, Real J A, Tuchagues J P, Dennis A C and Boillot M L 2000 *Chem. Phys. Lett* **318** 409
[33] Adler P, Spiering H and Gütlich P 1987 *Inorg. Chem.* **26** 3840

[34] Bousseksou A, Verelst M, Constant-Machado H, Lemercier G, Tuchagues J P and Varret F 1996 *Inorg. Chem.* **35** 110
[35] Doniach S 1978 *J. Chem. Phys.* **68** 11
[36] Shteto I, Boukheddaden K and Varret F 1999 *Phys. Rev.* E **60** 5139
[37] Boukheddaden K, Shteto I, Hoo B and Varret F 2000 *Phys. Rev.* B **62** 14 806
[38] Adler P, Hauser A and Gütlich P 1988 *Chem. Phys. Lett.* **152** 468
[39] Hauser A, Romstedt H and Spiering H 1998 *3rd Spin Crossover Family Meeting (Seeheim, Germany)* results presented
[40] Hoo B, K Boukheddaden and Varret F 2000 *Eur. Phys. J.* B **17** 449
[41] Roubeau O, Haasnoot J G, Linarès J and Varret F 1999 *Proc. ICMM '98 (Seignosse, France); Mol. Cryst. Liq. Cryst.* **335** 541
[42] Hauser A, Jeftic J, Romstedt H, Hinek R and Spiering H 1999 *Coord. Chem. Rev.* **190–192** 471
[43] Codjovi E, Morscheidt W, Jeftic J, Linarès J, Nogués M, Goujon A, Roubeau O, Constant-Machado H, Desaix A, Bousseksou A, Verdaguer M and Varret F 1999 *Proc. ICMM '98 (Seignosse, France); Mol. Cryst. Liq. Cryst.* **335** 1295
[44] Enachescu C, Constant-Machado H, Codjovi E, Linarès J and Varret F 2001 *J. Phys. Chem. Solids* submitted
[45] Boukheddaden K, Linarès J, Spiering H and Varret F 2000 *Eur. Phys. J.* B **15** 317
[46] Bukhs E, Navon G, Bixon M and Jortner J 1980 *J. Am. Chem. Soc.* **102** 2918
[47] Jeftic J and Hauser A 1996 *Chem. Phys. Lett.* **248** 458
Jeftic J and Hauser A 1997 *J. Chem. Phys.* B **101** 10 262
[48] Spiering H 1997 *Z. Phys.* B **102** 455
[49] Linarès J, Spiering H and Varret F 1999 *Eur. Phys. J.* B **10** 271
[50] Ogawa Y, Koshihara S, Koshino K, Ogawa T, Urano C and Takagi H 2000 *Phys. Rev. Lett.* **84** 3181
[51] McGarvey J J and Lawthers I 1982 *J. Chem. Soc., Chem. Commun.* 904